Progress of Theoretical Physics, Vol. 67, No. 5, May 1982

General Relativistic Collapse of Non-Rotating, Axisymmetric Stars

Takashi NAKAMURA and Humitaka SATO

Research Institute for Fundamental Physics
Kyoto University, Kyoto 606

(Received November 13, 1981)

Numerical calculations have been made for the general relativistic collapse of non-rotating, axisymmetric stars of $10M_\odot$. The initial density of a star is about 3×10^{13} g/cm^3. As an equation of state, we use γ (adiabatic index)$=4/3$ for $\rho\leqq3\times10^{14}$ g/cm^3 and $\gamma\to2$ for $\rho\to\infty$. Both prolate and oblate collapse are calculated. It is suggested that Schwarzschild black holes may be formed if U (the ratio of the initial internal energy to the initial gravitational energy) $\gtrsim2/3$. If $U\lesssim2/3$, it is suggested that naked singularities may be formed for large initial deformation of stars.

§ 1. Introduction

Under the cosmic censorship hypothesis[1] the Schwarzschild metric is known to be unique as the ultimate space-time of the gravitational collapse of non-rotating stars.[2] In fact, the other asymptotically flat static metrics have a naked singularities, which was discussed by Zipoy[3] and Voorhees[4] for some special class of Weyl metric.[5),6] However all these studies were restricted to vacuum space-times. In a realistic situation a star collapses from a state of weak gravity into a state of strong gravity. Only the study of such a dynamical process can give us the final state of non-spherical, and non-rotating stars.

For spherically symmetric cases, Yodzis et al.[7] showed a possibility of existence of a naked singularity. For non-rotating, axisymmetric cases, Nakamura et al.[8] suggested that a naked singularity may appear in a prolate collapse if initial quadrupole moment is large enough. However in the above two cases, pressure is zero or ineffective for $\rho\to\infty$. In this paper, we calculate collapse of non-rotating stars of $10M_\odot$ with a realistic equation of state. In § 2, the initial conditions and the coordinate conditions are shown. In § 3, numerical results are shown. In § 4, we give some discussions.

§ 2. Basic equations

We adopt the cylindrical coordinates (R, Z, ϕ). We assume the system is axially symmetric and is plane symmetric about $Z=0$ plane. In the non-rotating cases, the $[(2+1)+1]$-formalism of the Einstein equations[9] is equivalent to the $(3+1)$-formalism.[10] Since a full set of the Einstein equations for the present case

can be easily given from the previous paper[11] (Paper I), dropping the terms related to rotation, we do not write them here. Units of mass, length and time are taken as

$$M=10M_{\odot}\,, \qquad L=GM/c^2 \quad \text{and} \quad T=GM/c^3\,. \tag{1}$$

The basic flow of the numerical calculations and the basic ideas of the finite difference method are found by Nakamura et al.[12] and in Paper I.

1) *Initial conditions*

We assume there is no poloidal motion at $t=0$. The initial 3-space metric is assumed to be conformally flat,

$$\gamma_{ij}=\phi^4(\gamma_{ij})_{\text{flat}}\,, \tag{2}$$

where ϕ is the conformal factor. ϕ is determined by the Hamiltonian constraint equation,

$$(\Delta_{\text{flat}})\phi=-2\pi(\rho_H\phi^6)/\phi\,, \tag{3}$$

where ρ_H is the energy density measured by the observer whose four velocity is the normal vector of $t=$const hypersurface. As ρ_H, we use the form,

$$\rho_H\phi^6=\frac{1}{(2\pi)^{3/2}a^2b}\exp\left(-\frac{R^2}{2a^2}-\frac{Z^2}{2b^2}\right) \tag{4}$$

and

$$a^2b=(1.5)^3\,.$$

The method of solving Eq. (3) under the condition of Eq. (4) is given in Ref. 12).

As an equation of state, we use

$$\begin{aligned} p&=1/3\rho\varepsilon && \text{for } \rho\leqq\rho^*\equiv 3\times10^{14}\ \text{g/cm}^3=0.05 \text{ in our units}\,,\\ &=(\rho-\rho^*)\varepsilon+\frac{1}{3}\rho^*\varepsilon && \text{for } \rho>\rho^*\,, \end{aligned} \tag{5}$$

where p, ρ and ε are pressure, proper mass density and internal energy per unit mass, respectively. Equation (5) will mimic the equation of state given by Lamb et al.[13] For $\rho\leqq\rho^*$, the trapped leptons play a major role in the pressure. For $\rho>\rho^*$, nuclear force is taken into account by the first term on the r.h.s. of Eq. (5). The sound velocity approaches the light velocity for $\rho\to\infty$, which is the causality limit.[14] The initial distribution of ε is taken as

$$\varepsilon=K\rho^{1/3}\,, \tag{6}$$

where K is a constant.

Now a and K determine the initial conditions uniquely. Instead of K, we use U defined by

$$U = E_{\rm int}/|E_{\rm grav}|, \tag{7}$$

where $E_{\rm int}$ and $E_{\rm grav}$ are the initial internal energy and the initial gravitational energy, respectively (see Paper I).

2) *Coordinate conditions*

The shift vector is taken to be zero. Therefore the coordinate line agrees with the normal line to the t=constant hypersurface. As for the lapse function, the maximal slicing condition is used in almost all models. Some of the models have been recalculated by using the hypergeometric slicing condition defined in Paper I.

§ 3. Numerical results

In all the numerical calculations the number of grids is 28×28. The coordinate of the outermost grid point is (25, 25). In Table I, the initial parameters of each model are shown. For each model, we have tried to identify an apparent horizon using the method given by Sasaki et al.[15] In Fig. 1, we show whether the apparent horizon is identified or not for each model in the U-a plane. In this figure, the circles mean that the apparent horizon is identified and crosses not identified. In the following, we shall describe some details of four typical models; two prolate and two oblate cases. The name of the model is given in Table I.

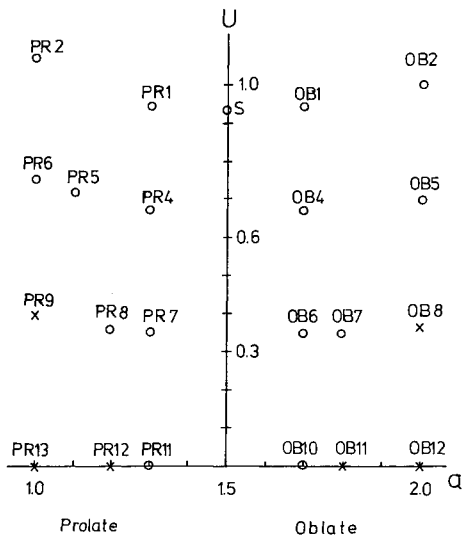

Fig. 1. The initial parameters of each model in the U-a plane. Circles mean that apparent horizons are identified. Crosses mean that they are not.

(i) Model PR2

In this model, the initial internal energy is close to the virial value. At the beginning, a thin envelope expands toward the lateral direction. In the central region, the collapse occurs in a rather spherically symmetric way. In the region where $Z\simeq4$ and $R\lesssim2$, the matter collapses almost vertically as seen in Fig. 2(a). The thin envelope continues to expand. In the center, the collapse proceeds (Fig. 2(b)). At

Table I. The initial parameters of each model. PR and OB imply the prolate and the oblate initial density distribution, respectively. In the fourth column, Max means the maximal slicing and Hyper means the hypergeometric slicing defined in Paper I.

Model Name	U	a	Time Slice	Apparent Horizon?
S	0.93	1.5	Max	YES
PR1	0.95	1.3	Max	YES
PR2	1.08	1.0	Max	YES
OB1	0.94	1.7	Max	YES
OB2	0.99	2.0	Max	YES
PR3	2.2	0.5	Max	NO
OB3	1.7	4.0	Max	NO
PR4	0.67	1.3	Max	YES
PR5	0.72	1.1	Max	YES
PR6	0.76	1.0	Max	YES
OB4	0.67	1.7	Max	YES
OB5	0.70	2.0	Max	YES
PR7	0.36	1.3	Max	YES
PR8	0.37	1.2	Max	YES
PR9	0.40	1.0	Max	NO
PR10	0.40	1.0	Hyper	NO
OB6	0.35	1.7	Max	YES
OB7	0.35	1.8	Max	YES
OB8	0.37	2.0	Max	NO
OB9	0.37	2.0	Hyper	NO
PR11	0.	1.3	Max	YES
PR12	0.	1.2	Max	NO
PR13	0.	1.0	Max	NO
OB10	0.	1.7	Max	YES
OB11	0.	1.8	Max	NO
OB12	0.	2.0	Max	NO

$t=14.3$, the collapse along the lateral direction is decelerated and the matter falls almost vertically in the central region (Fig. 2(c)). Finally, the matter distribution becomes almost spherically symmetric in our coordinates and an apparent horizon is formed (Fig. 2(d)).

(ii) Model PR9

The initial density distribution of this model is the same as that of Model PR2. As the initial internal energy is 0.37 times that of Model PR2, we do not see any expansion of a thin envelope (Fig. 3(a)) contrary to Fig. 2(a). The collapse along the lateral direction is not decelerated (Fig. 3(b)). At $t=14.3$, the matter

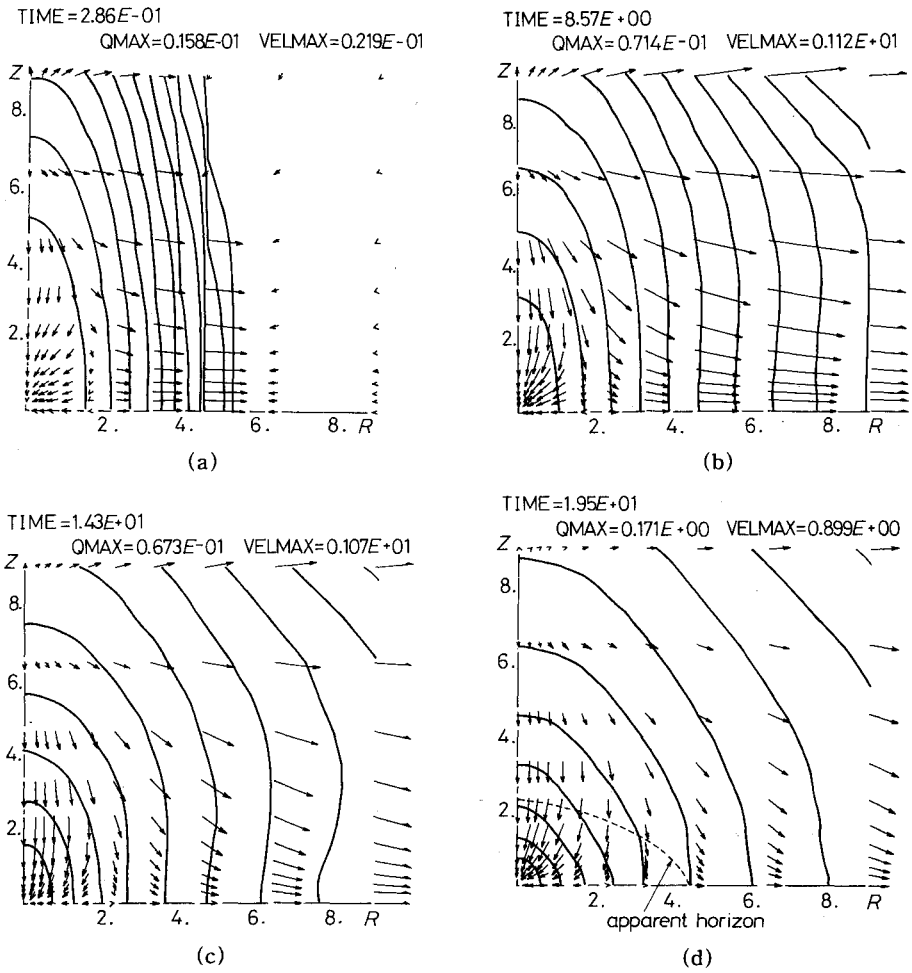

Fig. 2. Contour lines of Q_b for PR2. The space integral of Q_b becomes the total rest mass (M_B), that is, $2\pi\int_{-\infty}^{\infty}\int_{0}^{\infty} Q_b R dR dZ = M_B$. The precise definition of Q_b can be found in Paper I. Each line corresponds to $Q_b = \mathrm{QMAX}\cdot 10^{-n/2}$ for $n=1, 2, \cdots, 11$. QMAX is shown in the figure. Arrows show the space component of the four velocity of the fluid. The maximum of the velocity is shown in the figure as VELMAX. In Fig. 2(d), the dashed line shows the apparent horizon.

falls mainly along the lateral direction (Fig. 3(c)), which is completely contrary to Fig. 2(c). Finally, the matter distribution becomes rod-like (Fig. 3(d)). The apparent horizon has not been identified up to the final stage of the computation by using the maximal slicing. Then, we have recalculated this model by using the hypergeometric slicing defined in Paper I. Even in this case of Model PR10, the apparent horizon has not been identified.

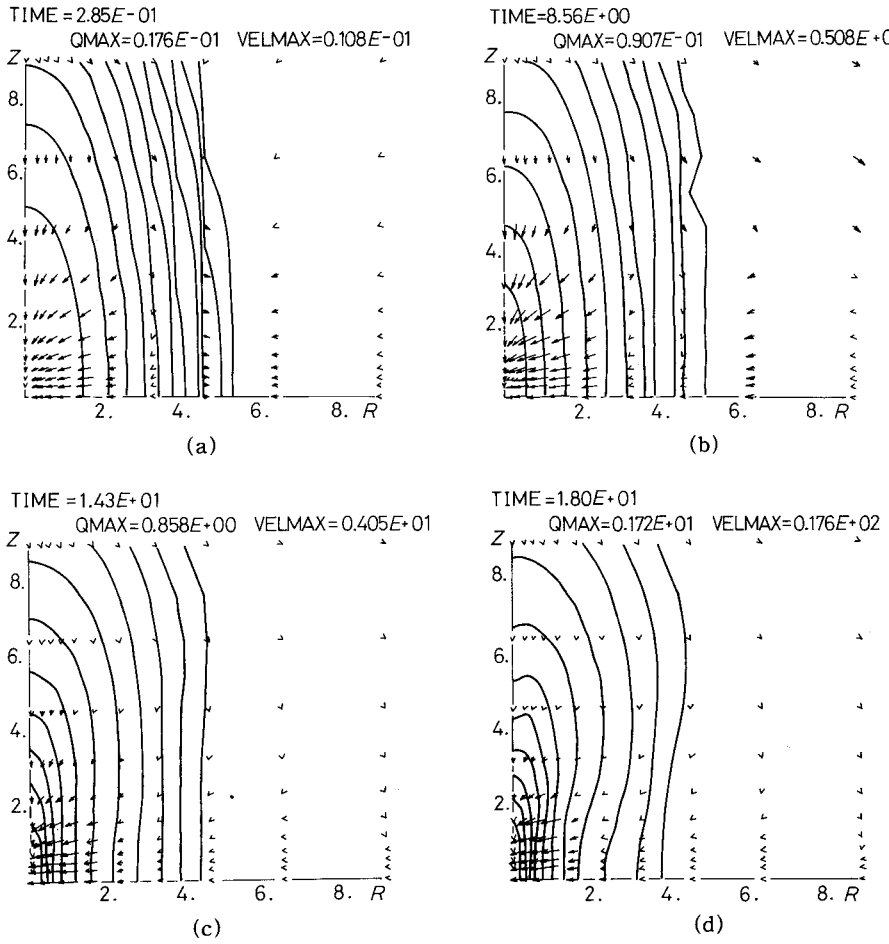

Fig. 3. Contour lines of Q_b for PR9. The notations are the same as those in Figs. 2(a)~(d).

(iii) Model OB2

In this model, the initial internal energy is close to the virial value. At the beginning, a thin envelope expands. At the center, the collapse is almost spherically symmetric. In the region where $R \simeq 2$ and $Z \lesssim 1.5$, the matter falls along the lateral direction (Fig. 4(a)). The thin envelope continues to expand, but, in the central region, the matter collapses almost along the lateral direction (Fig. 4(b) and (c)). Finally, the matter distribution becomes slightly prolate and the apparent horizon is formed (Fig. 4(d)).

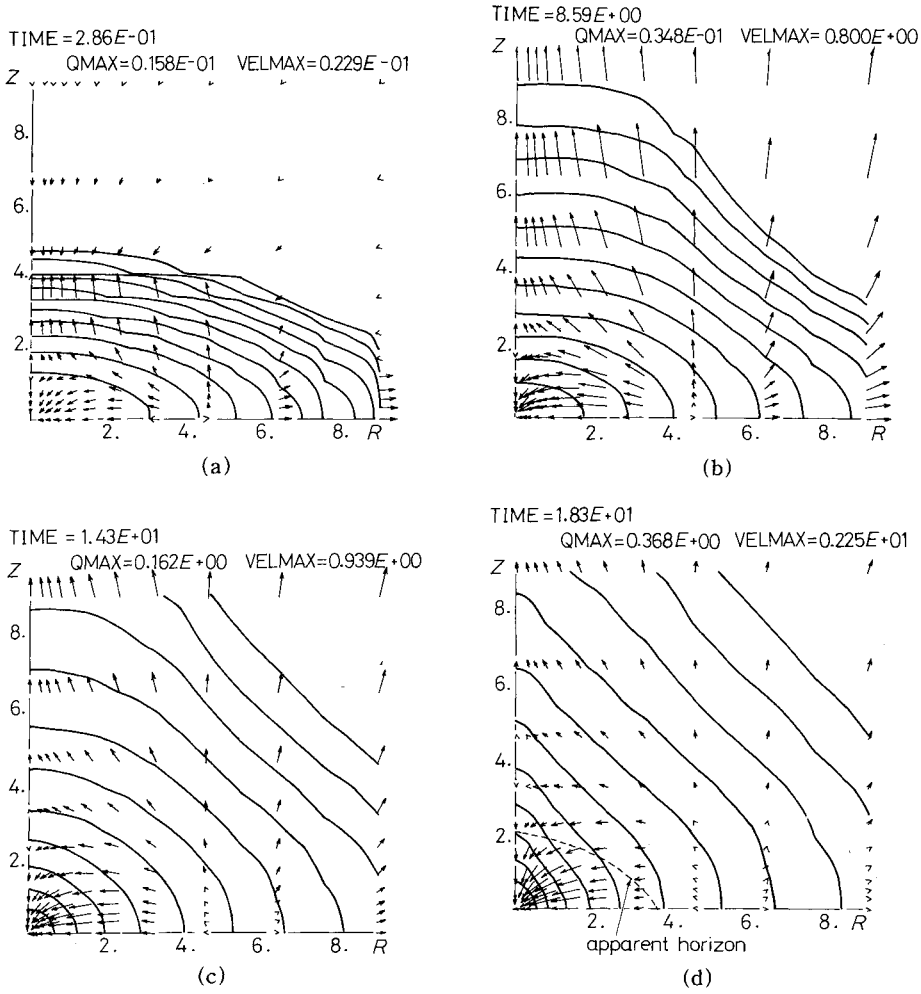

Fig. 4. Contour lines of Q_b for OB2.

(iv) Model OB8

The initial internal energy of this model is 0.37 times that of Model OB2. The thin envelope does not expand because of small pressure force (Fig. 5(a)). The matter falls both in Z- and R-direction (Figs. 5(b) and (c)). Finally the density distribution becomes disk-like. In this model the apparent horizon has not been identified. Even in Model OB9, which is calculated by using the hypergeometric slicing, the apparent horizons has not been identified.

For zero internal energy models, the features are the same as those of PR9 and OB8. For the models PR13 and PR12, the matter distribution becomes rod-

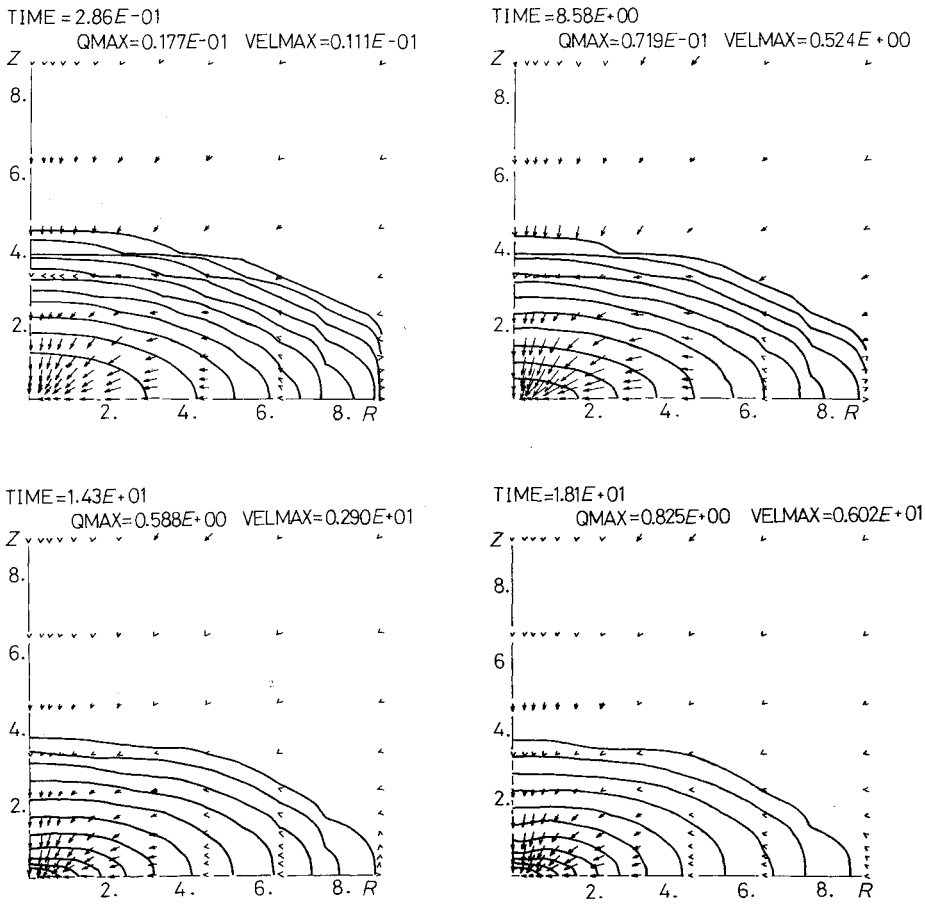

Fig. 5. Contour lines of Q_b for OB8.

like and for the models OB11 and OB12, it does disk-like. For the models PR11 and OB10, although the density distribution is deformed in our coordinates, the apparent horizons are formed. For the other nonzero internal energy models, their features are in between the models discussed above and the spherical model S. If the initial internal energy is too large, as in the models PR3 and OB3, a star expands and the apparent horizon is not formed. As these models are not interesting, we shall not comment further.

§ 4. Concluding remarks and discussion

As seen from Fig. 1 and the results given in § 3, the density distribution

becomes almost spherically symmetric in our coordinates in the final stage if $U \gtrsim 2/3$ and the apparent horizon is formed even if the distribution is strongly deformed at the beginning. In all the models with $U \gtrsim 2/3$, we have found that nothing peculiar occurs outside the apparent horizon. If we recall that the singularity of the Schwarzschild black hole is hidden by the event horizon, our numerical results suggest that the Schwarzschild black holes may be formed for the collapse of a non-rotating and axisymmetric star if $U \gtrsim 2/3$.

If $U \lesssim 2/3$, our results show that the initial deformation of the density distribution is amplified to rod-like or disk-like distribution and the apparent horizon is not formed. If we recall the structure of the Weyl metric which does not have the event horizon, but has the rod-like or the disk-like naked singularities, the above models with $U \lesssim 2/3$ may evolve to one of Weyl's solutions. However such a low U model may not be realistic. A star should have evolved in a quasistatic manner until the instability to the collapse sets in. Therefore, its internal energy at the beginning of the collapse may be close to the virial value, that is, $U=1$ in our equation of state.

One of the present authors (T.N.) calculated the general relativistic collapse of rotating stars of $10M_{\odot}$.[11] The present authors have calculated the general relativistic collapse of rotating supermassive stars.[16] From these results, we suggested that the Kerr black holes may be formed for wide ranges of the initial conditions provided that the initial density and angular velocity decreases uniformly with radius.[17] If we note the Schwarzschild metric is the special case of the Kerr metric, the present numerical results and the previous numerical results[17] enforce the following prediction: In the general relativistic collapse of *axially* symmetric stars, the Kerr black holes may be formed for wide ranges of the *plausible* initial conditions.

The authors would like to thank Professor C. Hayashi for his continuous encouragement. This work was supported by the Scientific Research Fund of the Ministry of Education, Science and Culture (564123). One of the authors (T.N.) is indebted to Soryushi Shogakukai for the financial aid.

References

1) R. Penrose, Ann. N. Y. Acad. Sci. **224** (1973), 125.
2) W. Israel, Phys. Rev. **164** (1967), 1776.
3) D. M. Zipoy, J. Math. Phys. **7** (1966), 1137.
4) B. H. Voorhees, Phys. Rev. **D2** (1970), 2119.
5) H. Weyl, Ann. der Physik **54** (1917), 117.
6) T. Levi Civita, Atti. Acad. Naz. Lincei **5** (1917), 26.
7) P. Yodzis, H. J. Seifert and Müller zum Hagen, Comm. Math. Phys. **34** (1973), 135.
8) T. Nakamura, K. Maeda, S. Miyama and M. Sasaki, *Proceedings of the Second Marcel Grossmann Meeting on General Relativity* (North-Holland, Amsterdam, 1981).
9) K. Maeda, M. Sasaki, T. Nakamura and S. Miyama, Prog. Theor. Phys. **63** (1980), 719.

10) R. Arnowitt, S. Deser and C. W. Misner, "The Dynamics of General Relativity" in *Gravitation; An Introduction to Current Research* (1962), ed. L. Witten (Wiley, New York, 1962), p. 227.
11) T. Nakamura, Prog. Theor. Phys. **65** (1981), 1876.
12) T. Nakamura, K. Maeda, S. Miyama and M. Sasaki, Prog. Theor. Phys. **63** (1980), 1229.
13) D. Q. Lamb, J. M. Lattimer, C. J. Pethick and D. G. Ravenhall, Phys. Rev. Letters **41** (1978), 1623.
14) Ya. B. Zel'dovich, Soviet Phys. JETP **14** (1962), 1143.
15) M. Sasaki, K. Maeda, S. Miyama and T. Nakamura, Prog. Theor. Phys. **63** (1980), 1051.
16) T. Nakamura and H. Sato, Prog. Theor. Phys. **66** (1981), 2038.
17) T. Nakamura and H. Sato, Phys. Letters **A86** (1981), 318.